Supporting Information

A protease-activated, near-infrared fluorescent probe for
early endoscopic detection of premalignant gastrointestinal lesions

Authors

Joshua J. Yim[1]*, Stefan Harmsen[2,3]*, Krzysztof Flisikowski[4], Tatiana Flisikowska[4], Hong Namkoong[5], Megan Garland[6], Nynke S. van den Berg[7], José G. Vilches-Moure[8], Angelika Schnieke[4], Dieter Saur[9-11], Sarah Glasl[12,13], Dimitris Gorpas[12,13], Aida Habtezion[5], Vasilis Ntziachristos[12,13], Christopher H. Contag[14], Sanjiv S. Gambhir[2,15,16,†], Matthew Bogyo[1,17,18,#], Stephan Rogalla[2,5,#]

*equal contribution, †Deceased July 18, 2020

Affiliations

[1]Department of Chemical and Systems Biology, Stanford University School of Medicine, Stanford, CA, USA

[2]Department of Radiology, Bio-X Program and Molecular Imaging Program at Stanford University (MIPS), Stanford University School of Medicine, Stanford, CA, USA

[3]Department of Radiology, Perelman School of Medicine at the University of Pennsylvania, Philadelphia, USA

[4]Chair of Livestock Biotechnology, Technische Universität München, Freising, Germany

[5]Department of Medicine, Division of Gastroenterology & Hepatology, Stanford University School of Medicine, Stanford, CA, USA

[6]Department of Cancer Biology, Stanford University School of Medicine Stanford, CA, USA

[7]Department of Otolaryngology – Head and Neck Surgery, Stanford University School of Medicine, Stanford, CA, USA

[8]Department of Comparative Medicine, Stanford School of Medicine, Stanford, CA, USA

[9]Division of Translational Cancer Research, German Cancer Research Center (DKFZ) and German Cancer Consortium (DKTK), Heidelberg, Germany

[10]Chair of Translational Cancer Research and Institute for Experimental Cancer Therapy, Klinikum rechts der Isar, School of Medicine, Technische Universität München, Munich, Germany

11Department of Internal Medicine II, Klinikum rechts der Isar, Technische Universität München, Munich, Germany

12Helmholtz Zentrum München, German Research Center for Environmental Health, Institute of Biological and Medical Imaging, Neuherberg, Germany

13Chair of Biological Imaging, TranslaTUM, Technische Universität München, Munich, Germany

14Department of Biomedical Engineering, Institute for Quantitative Health Science and Engineering, Michigan State University, East Lansing, MI, USA

15Department of Bioengineering, Department of Materials Science & Engineering Stanford University, Stanford, CA, USA

16Canary Center at Stanford for Early Cancer Detection, Palo Alto, CA, USA

17Department of Pathology, Stanford University School of Medicine, Stanford, CA, USA

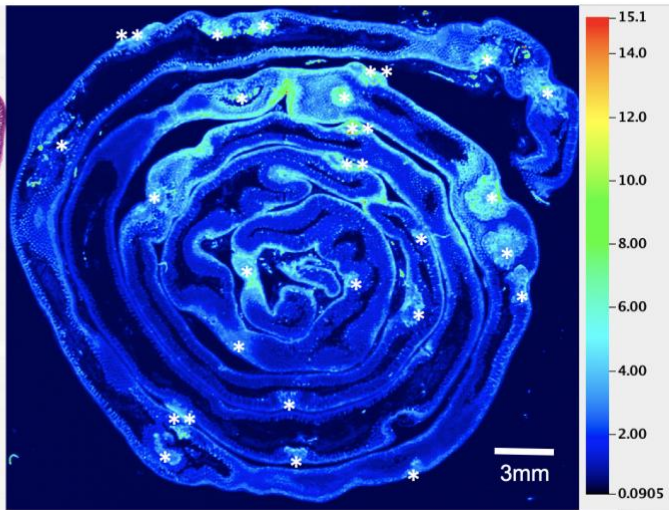18Department of Microbiology and Immunology, Stanford University School of Medicine, Stanford, CA, USA

The authors declare no competing interest.

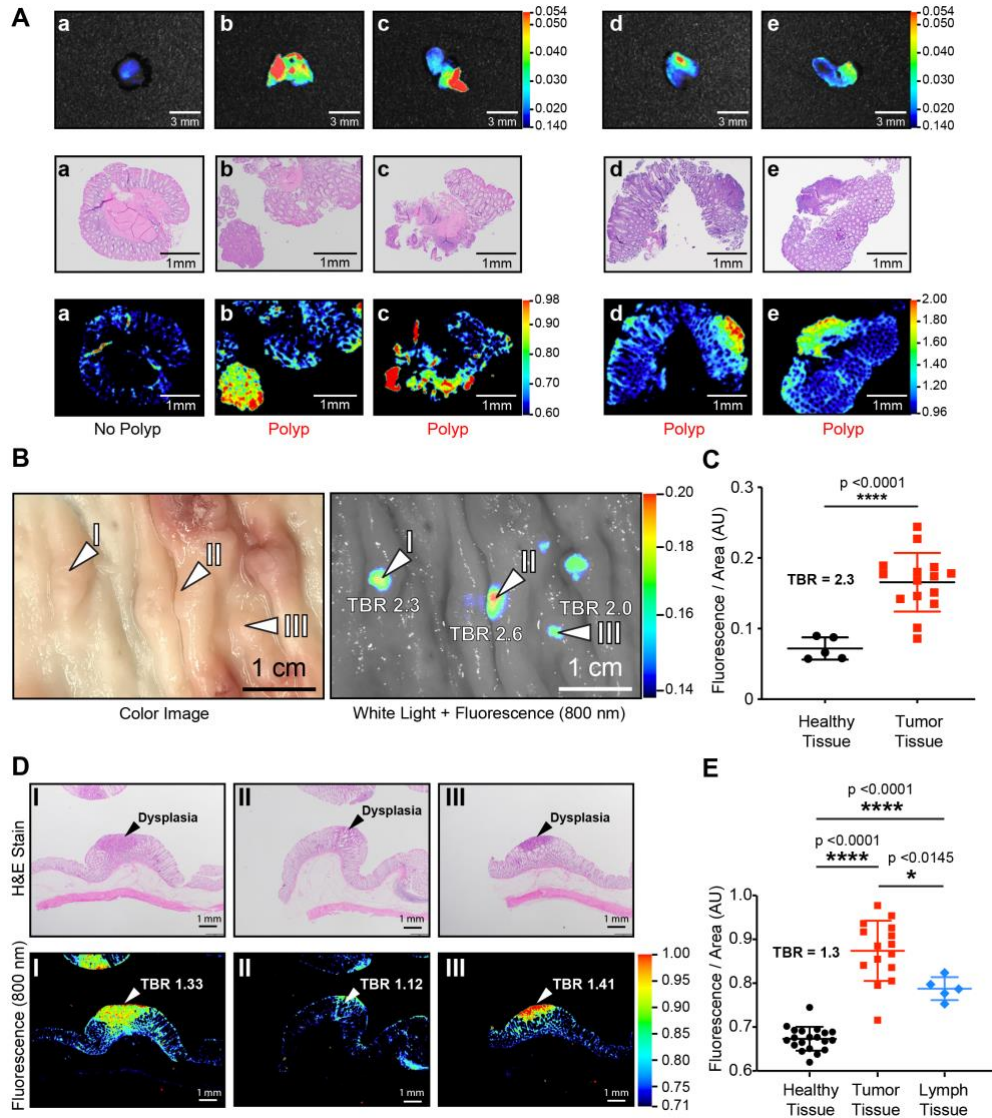#To whom correspondence may be addressed. Email: srogalla@stanford.edu or mbogyo@stanford.edu
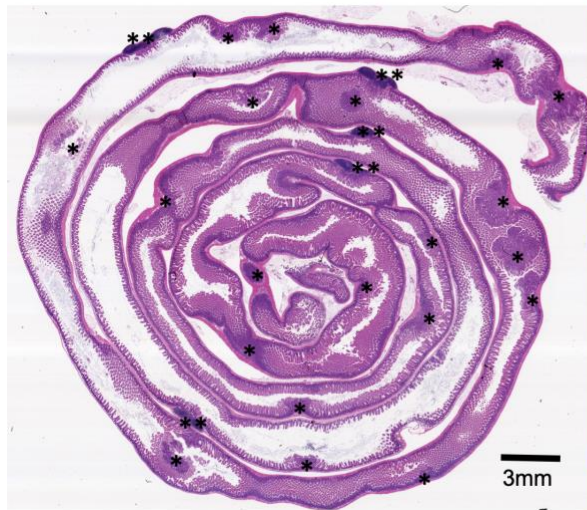
Supplemental Figure 1. **NIRF Imaging of colorectal carcinogenesis in *Apc^min/+* mice using 6QC-ICG**. H&E stained slide from tissue section deeper within the tissue block from **Figure 2**. (*) identified as adenoma; (**) identified as gut-associated lymphoid tissue (GALT).

Supplemental Figure 2. **NIRF-guided biopsy in porcine model of colorectal carcinogenesis with 0.25 mg/kg dose of 6QC-ICG.** (A) Top row shows wide-field NIRF images of tissues obtained during NIRF-guided biopsy. The middle row shows corresponding H&E stained tissue of biopsied tissue and confirms the histological status of the tissues. (B) Images and tissue scans of colon tissue from an $APC^{1311/+}$ porcine model injected IV with **6QC-ICG** (sacrificed at 24 h PI, 0.25 mg/kg). Wide-field imaging with white-light (top) and corresponding 800 nm fluorescence image (bottom). (C) Colon tissue slices stained with H&E (top) and their corresponding flat-bed imager 800 nm scans (bottom). (D) Quantification of fluorescence signals of healthy and tumor tissue from wide field imager for $APC^{1311/+}$pig injected with 0.25 mg/kg of probe. (E) Quantification of fluorescence of healthy, tumor, and lymph sections of scanned colon tissue taken from the $APC^{1311/+}$pigs injected with 0.25 mg/kg of probe. Error bars are standard deviation.

SI Appendix Figure 3 – Calculation of performance of 6QC-ICG

Fig 2. *Apc^{min/+}* Mice

A. True Positive = 19
B. False Positive = 1
C. False Negative = 1
D. True Negative = 15

- Sensitivity = 19/20 = 95.0%
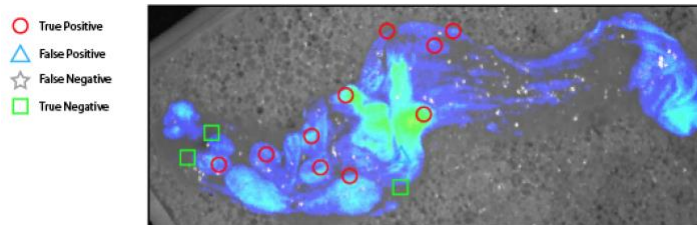- Specificity = 15/16 = 93.8%
- Precision = 19/20 = 95.0%
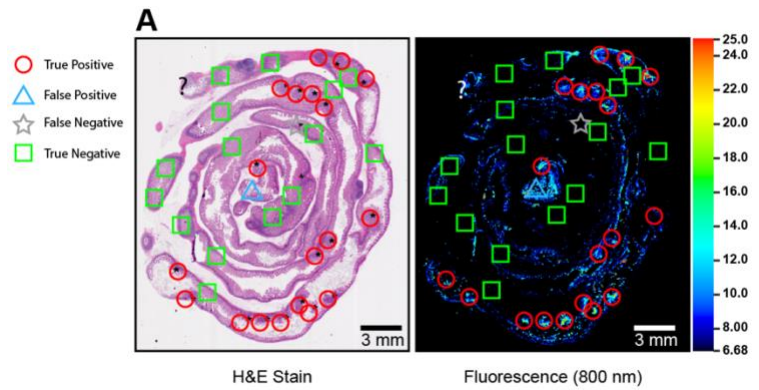
Fig 4. *APC^{1311/+}* Pig Colon (1.0 mg/kg)

A. True Positive = 17
B. False Positive = 0
C. False Negative = 0
D. True Negative = 3

- Sensitivity = 17/17 = 100%
- Specificity = 3/3 = 100%
- Precision = 17/17 = 100%
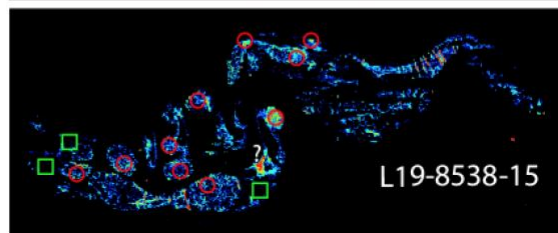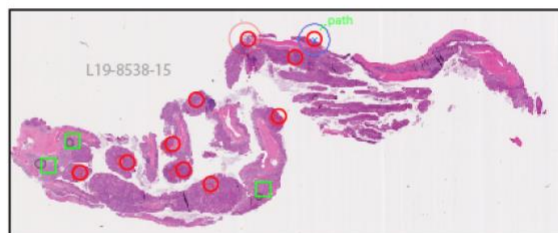
Fig 4 SI. Pig Colon (0.25 mg/kg)

A. True Positive = 14
B. False Positive = 1
C. False Negative = 1
D. True Negative = 4

- Sensitivity = 14/15 = 93.3%
- Specificity = 4/5 = 80.0%
- Precision = 14/15 = 93.3%

Fig 5. HET AOM-DSS

A. True Positive = 10
B. False Positive = 0
C. False Negative = 0
D. True Negative = 3

- Sensitivity = 10/10 = 100%
- Specificity = 3/3 = 100%
- Precision = 10/10 = 100%

SI Appendix Video 1

Video screen capture of WL/NIRF endoscopic surveillance in Apc$^{Pirc/+}$ rat with **6QC-ICG** treatment (18 h PI, 1.2 mg/kg). **Left:** White light (WL) video imaging with near-infrared fluorescence (NIRF) detector in yellow. **Right:** Corresponding NIRF video imaging corresponding to polyps found in WL imaging.

SI Appendix Video 2

Video screen capture of WL/NIRF endoscopic surveillance in APC$^{1311/+}$ pig with **6QC-ICG** treatment (18 h PI, 1.0 mg/kg). **Top left:** White light (WL) video imaging. **Bottom Left:** Corresponding near-infrared fluorescence (NIRF) video imaging. **Right:** Overlay merge of WL and NIRF video.